

Research Article

Medullary Thyroid Carcinomas Classified According to the International Medullary Carcinoma Grading System and a Surveillance, Epidemiology, and End Results-Based Metastatic Risk Score: A Correlation With Genetic Profile and Angioinvasion

Federica Torricelli^a, Giacomo Santandrea^{b,c}, Cecilia Botti^c, Moira Ragazzi^{b,d}, Silvia Vezzani^e, Andrea Frasoldati^e, Angelo Ghidini^f, Davide Giordano^f, Eleonora Zanetti^b, Teresa Rossi^a, Davide Nicoli^g, Alessia Ciarrocchi^{a,*}, Simonetta Piana^{b,*}

^a Laboratory of Translational Research, Azienda USL-IRCCS di Reggio Emilia, Reggio Emilia, Italy; ^b Pathology Unit, Azienda USL-IRCCS di Reggio Emilia, Reggio Emilia, Italy; ^c Clinical and Experimental Medicine PhD Program, University of Modena and Reggio Emilia, Modena, Italy; ^d Department of Medical and Surgical Sciences for Children and Adults, University of Modena and Reggio Emilia, Modena, Italy; ^e Endocrinology Unit, Azienda USL-IRCCS di Reggio Emilia, Reggio Emilia, Italy; ^f Otolaryngology Unit, Azienda USL-IRCCS di Reggio Emilia, Reggio Emilia, Italy; ^g Laboratory of Molecular Pathology, Azienda USL-IRCCS di Reggio Emilia, Reggio Emilia, Italy

ARTICLE INFO

Article history:

Received 16 February 2023
Revised 17 May 2023
Accepted 5 June 2023
Available online 10 June 2023

Keywords:

classification
medullary carcinoma
prognosis
thyroid

ABSTRACT

Due to the lack of a standardized tool for risk-based stratification, the International Medullary Carcinoma Grading System (IMTCGS) has been proposed for medullary thyroid carcinomas (MTCs) based on necrosis, mitosis, and Ki67. Similarly, a risk stratification study using the Surveillance, Epidemiology, and End Results (SEER) database highlighted significant differences in MTCs in terms of clinical-pathological variables. We aimed to validate both the IMTCGS and SEER-based risk table on 66 MTC cases, with special attention to angioinvasion and the genetic profile. We found a significant association between the IMTCGS and survival because patients classified as high-grade had a lower event-free survival probability. Angioinvasion was also found to be significantly correlated with metastasis and death. Applying the SEER-based risk table, patients classified either as intermediate- or high-risk had a lower survival rate than low-risk patients. In addition, high-grade IMTCGS cases had a higher average SEER-based risk score than low-grade cases. Moreover, when we explored angioinvasion in correlation with the SEER-based risk table, patients with angioinvasion had a higher average SEER-based score than patients without angioinvasion. Deep sequencing analysis found that 10 out of 20 genes frequently mutated in MTCs belonged to a specific functional class, namely chromatin organization, and function, which may be responsible for the MTC heterogeneity. In addition, the genetic signature identified 3 main clusters; cases belonging to cluster II displayed a significantly higher number of mutations and higher tumor mutational burden, suggesting increased genetic instability, but cluster I was associated with the highest number of negative events. In conclusion, we confirmed the prognostic performance of the IMTCGS and SEER-based risk score, showing that patients classified as high-grade had a lower event-free survival

These authors contributed equally: Federica Torricelli and Giacomo Santandrea.

* Corresponding authors.

E-mail addresses: simonetta.piana@ausl.re.it (S. Piana), alessia.ciarrocchi@ausl.re.it (A. Ciarrocchi).



probability. We also underline that angioinvasion has a significant prognostic role, which has not been incorporated in previous risk scores.

© 2023 United States & Canadian Academy of Pathology. Published by Elsevier Inc. All rights reserved.

Introduction

Medullary thyroid carcinomas (MTCs) account for about 2% of all thyroid malignancies and are characterized by a variable degree of aggressiveness. MTCs can occur either as sporadic disease or as part of hereditary genetic syndromes associated with distinctive germline alterations in the *RET* gene. Tumor stage is a well-known strong predictor of survival, with metastatic disease having a more dramatic outcome than lesions confined to the primary site.^{1–4} On the other hand, a grading system has not been definitively accepted, even though certain cyto-histologic findings, such as cytologic features, nuclear pleomorphism, mitosis, and amyloid deposits, have long been investigated as potential prognostic parameters.

To address the lack of a standardized tool for risk-based stratification, the International Medullary Carcinoma Grading System (IMTCGS) was proposed as a universal grading system for MTCs in 2021.⁵ This system merges 2 different grading schemes, one from the Memorial Sloan Kettering Cancer Center in New York, United States,⁶ and the other from the Royal North Shore Hospital in Sydney, Australia,⁷ and has been implemented by members of both institutions. The system takes into account 3 main histologic variables, including necrosis, mitotic count, and Ki67 proliferative index, with the aim to categorize MTCs into high- and low-risk tumors, thus anticipating clinical aggressiveness in line with the grading of other neuroendocrine tumors arising in the lung or the gastrointestinal tract.⁸ This 2-tiered system, which is easier to apply than a 3-tier classification system, is poised to be a powerful tool in managing MTC patients and has already been evaluated in recent papers with positive results. In fact, Vissio et al⁹ applied all 3 systems (IMTCGS, the Memorial Sloan Kettering Cancer Center grading system, and the Sydney grading system) to a cohort of 111 MTC patients and demonstrated the superiority of the IMTCGS in predicting MTC clinical behavior, although none of the grading systems showed a correlation with overall survival. Podany et al¹⁰ found that the distinction between low-grade and high-grade cases in a cohort of 59 MTC patients was helpful in prognostication. In addition, a recent metastatic risk study based on the Surveillance, Epidemiology, and End Results (SEER) database highlighted significant differences between MTCs in terms of clinical-pathological variables, including male sex, age, tumor size, extrathyroidal extension, and lymph node metastasis.¹¹ Evaluating 2526 MTC patients, the authors developed a risk table and identified 3 risk groups with significant survival differences to predict metastasis.

Recently, an “old-fashioned” morphologic feature, ie, angioinvasion, has been reevaluated to predict the metastatic potential of MTCs. Rios et al¹² and Erovcic et al¹³ found that angioinvasion at diagnosis is the main independent prognostic factor and the most reliable predictor of MTC recurrence, respectively.

In addition to histopathological parameters, identifying specific mutational fingerprints associated with the IMTCGS could help to consolidate its clinical application and provide additional refinements. In fact, little is known about the genetic landscape of MTCs. Although approximately 25% of patients with MTC will be carriers of MEN2 and somatic *RET* mutations (mostly the *RET*

p.M918T mutation), the latter has been reported in approximately half of the sporadic MTCs.^{14–16} In both cases, it is mandatory to identify either somatic or germline *RET* mutations to offer patients treatment with targeted *RET* inhibitors.¹⁷ Activating mutations in *RAS* (*H*-, *K*-, and *NRAS*) were reported in MTCs, although with a large frequency variability in different series. Interestingly, the occurrence of *RAS* and *RET* mutations exhibit a mutually exclusive pattern.^{18–23} A wide range of additional and mainly sporadic gene mutations, ie, *ALK* gene rearrangements,²⁴ was described by applying exome or targeted next-generation sequencing (NGS) on several cohorts, revealing a very heterogeneous and quite complex genetic background. Collectively, mutations in *RET* and *RAS* are the predominant alterations in MTCs, although their correlation with clinical behavior and prognosis is still controversial.

The purpose of the present study was threefold: (1) to validate the IMTCGS on a homogenous and well-characterized MTC cohort and compare it with the SEER-based risk table; (2) to investigate the potential prognostic role of other morphologic features, ie, angioinvasion; and (3) to study the genetic profile of MTCs in correlation with the IMTCGS and the SEER-based risk table.

Material and Methods

Patient Selection

The databases of the Pathology and Endocrinology units of the Santa Maria Nuova Hospital in Reggio Emilia were retrospectively searched to identify all patients who developed an MTC from 1980 to 2020. Complete clinical and surgical data, along with follow-up, were collected. All slides and blocks were retrieved from the Pathology archive. Once retrieved, cases were reviewed by 2 pathologists with a special interest in endocrine pathology (S.P. and G.S.), who reclassified the cases according to the 2022 World Health Organization (WHO) classification of thyroid neoplasms³ and staged them according to the eighth edition of the American Joint Committee on Cancer/Union for International Cancer Control (AJCC/UICC) TNM Classification of Malignant Tumors.

The most representative tumor blocks were selected for morphologic evaluation on hematoxylin and eosin, immunohistochemical evaluation of proliferative index with Ki67 antibody, and targeted molecular analysis.

Pathological Features

We evaluated several histologic parameters, including necrosis, architecture, cytology, desmoplasia, amyloid deposits, thyroid capsule infiltration, extrathyroidal extension, neoplastic angioinvasion, and lymph node status.

Specifically, necrotic areas were considered regardless of their extension; only ischemic foci morphologically ascribable to fine needle aspiration procedures were discarded. Mitotic counts were reported per 2 mm² starting from the areas of highest mitotic activity (ie, “hotspots”).²⁵ The mitotic index with Ki67 was calculated as strong nuclear staining in about 2000 cells.⁵

Angioinvasion was evaluated using already reported strict criteria²⁶ and considering only cell clusters intermingled with blood cells and fibrin, mainly placed in a subcapsular location. Although angioinvasion is no longer defined as focal or extensive in the latest WHO classification of endocrine tumors,³ we still preferred to define angioinvasion according to the number of foci involved to explore its potential role in tumor prognosis. All the cases were then graded according to the IMTCGS and the SEER-based metastatic risk stratification table.

Mutation Analysis

NGS libraries were prepared using the TruSight Oncology 500 DNA Kit (Illumina), starting from 40–500 ng of total DNA, following the manufacturer’s instructions. Sequencing was performed using the Illumina NextSeq 500 High Output Kit (2 x 101), providing a minimum of 50M reads per sample. Data were analyzed by the Local Run Manager TruSight Oncology 500 v2.2 Analysis Module (Illumina). Variants with a depth lower than 150 and minor allele frequency lower than 3% were excluded.

Germline variants were automatically excluded based on germline filters defined in the Illumina pipeline; the software initially excluded variants with an observed allele count ≥10 in any of the gnomAD and 1000 Genomes databases or variants with an allele frequency ≥90%. For the remaining variants, the software combined variants on the same chromosome with similar allele frequencies. The variant was removed if 5 or more similar variants were filtered in previously reported online databases.

Germline *RET* data were obtained by Sanger sequencing performed on blood samples after diagnosis. Assessment of germline *RET* mutation was routinely available starting from January 2000. Before 2000, *RET* mutation analysis was performed individually in an external research laboratory. The results of these analyses were not considered in our study and were considered “not available.”

Statistical Analysis

All analyses performed in this study were processed using the R software (v4.1.3). Mutation summary plots were generated using the R “maftools” package.²⁷ The association between genetic and clinical features was analyzed using Fisher exact test for categorical variables and the Kruskal-Wallis test for continuous variables.

The event-free survival (EFS) was computed as the time period from the date of surgery to the date of either recurrence/death or last follow-up. The survival analysis was performed using the log-rank test and Cox proportional hazards model. Kaplan-Meier curves were generated using the R “survminer” package. Associations and differences were considered statistically significant with a *P* value < .05.

Protein-protein interaction prediction was performed using the STRING tool and represented using the Cytoscape software.

Results

Patient Cohort

One hundred seventeen cases were found in the Pathology archives. Thirty-one cases were excluded because they were in consultation, and the paraffin blocks were unavailable. Slides and paraffin blocks were available for 86 patients; 20 cases failed the DNA and NGS quality check. The final cohort comprised 66 successfully profiled cases (44 females and 22 males; median age, 62 ranging from 12 to 84) (Fig. 1). The median follow-up of the entire cohort was 85 months.

Pathological Features

Most cases (53 out of 66, 80.3%) were represented by small, sharply demarcated intrathyroidal nodules; 13 cases had an

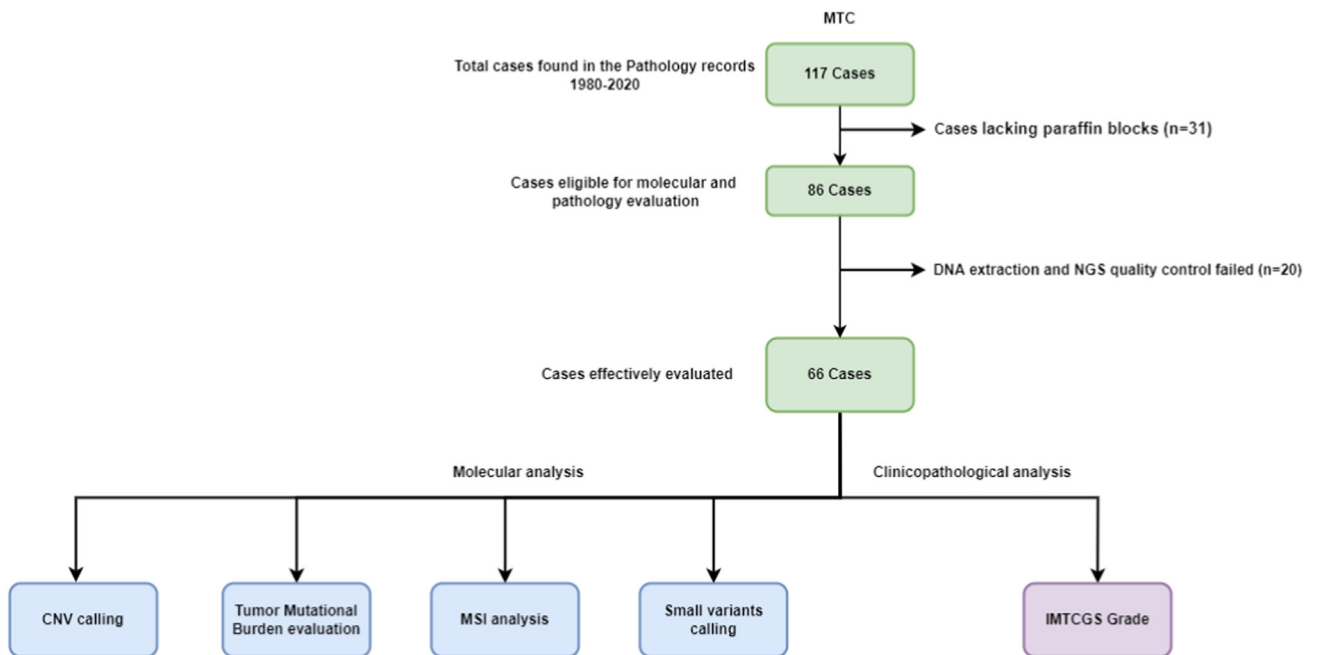


Figure 1. Flow diagram showing the cohort selection process.

infiltrative growth pattern. Fifty-four (81.8%) cases were represented by a single nodule, whereas the tumor was multifocal in 12 (18.2%) cases.

“Classic” neuroendocrine architecture (nested, trabecular, solid, and insular) was primarily observed (55 cases, 83.3%). Prominent zellballen-like nests were noted in 5 cases (7.5%). The remaining cases showed a “papillary-like” (2 cases, 3%), pseudoglandular (1 case, 1.5%), alveolar (1 case, 1.5%), or pleomorphic growth patterns (1 case, 1.5%).

Tumor cytology was conventional, with small, densely packed nuclei with salt-and-pepper chromatin in 45 cases (68.1%). A certain degree of nuclear pleomorphism, mostly focal, was noted in the remaining 21 cases (31.9%). Desmoplasia was absent in 32 cases (48.5%), focal in 25 cases (37.8%), and diffuse in 9 cases (13.6%). Amyloid deposits were not observed in 30 cases (45.5%), were focally present in 20 cases (30.3%), and were diffusely represented in 16 cases (24.2%).

We observed no angioinvasion in the majority of tumors (45 out of 66, 68.1%). One angioinvasion focus was observed in 9 cases (13.6%), 3 foci in 3 cases (4.5%), 4 foci in 5 cases (7.5%), and 5 foci in 4 cases (6.2%).

Thyroid capsule infiltration, without extrathyroidal extension, was present in 7 cases (10.6%) and absent in the remaining 59 (89.4%). Microscopic extrathyroidal invasion was largely absent (59 cases, 89.4%), with just 7 cases infiltrating the parathyroid tissue at presentation (10.6%). In most cases, surgical margins were visibly free (61 cases, 92.4%), whereas a complete surgical excision was not obtained in 5 cases.

The tumor size and extension according to the AJCC/UICC were pT1a in 22 patients (33.3%), pT1b in 22 patients (33.3%), pT2 in 17 patients (25.8%), pT3a in 1 patient (1.5%), and pT3b in 4 patients (6%). Lymph node status, according to the AJCC/UICC, was pN0 in 44 cases (66.6%), pN1a in 9 cases (13.7%), and pN1b in 13 cases (19.7%). The tumor stage, according to the AJCC/UICC, was stage I in 34 cases (51.5%), stage II in 10 cases (15.1%), stage III in 8 cases (12.1%), and stage IV in 14 cases (21.3%).

The status of germinal *RET* mutation was available in 26 MTCs (39.4%). Of these, 11 patients showed germline *RET* mutations (16.6%), and the remaining patients were wild-type. The pathological findings are summarized in [Supplementary Table S1](#).

International Medullary Carcinoma Grading System and Correlation With Surveillance, Epidemiology, and End Results-Based Risk Table

We applied grading criteria and evaluated the presence of necrosis, mitotic count in 2 mm² starting from a hotspot, and the Ki67 mitotic index according to the accepted best practice and the IARC recommendations.²⁵

Most cases were without identifiable necrotic foci (63, 95.5%). Diffuse or comedo-like necrotic foci were documented in only 3 cases (4.5%) ([Fig. 2A, D](#)). The mitotic index was <5 per 2 mm² in 65 cases, with just one case reaching the >5 mitoses per 2 mm² ([Fig. 2B, E](#)), and Ki67 was <5% in 47 cases (71.2%) and ≥5% in 19 cases (28.8%) ([Fig. 2C, F](#)).

According to the IMTCGS score criteria, 20 cases (30.3%) were classified as high-grade and 46 (69.7%) as low-grade ([Fig. 2G](#)). Among the 20 high-grade tumors, 17 had only 1 diagnostic feature, ie, a Ki67 > 5% (17 out of 20 cases, 85%). The remaining 3 cases had 2 diagnostic criteria, including 2 cases showing a Ki67 > 5% and tumor necrosis (10%), and 1 displayed a Ki67 > 5% and a mitotic index >5 per 2 mm². Notably, no cases showed all 3

diagnostic features, and a Ki67 > 5% was present in all high-grade cases ([Fig. 2H](#)).

Our cohort found a significant association between the IMTCGS and survival, showing patients classified as high-grade had a lower EFS probability than the low-grade MTCs ($P = .0047$) ([Fig. 3](#)). If we exclude pT1a cases, the correlation between IMTCGS and survival resulted in an even stronger significance ([Supplementary Fig. S1](#)).

Considering criteria other than those included in the grading scheme, angioinvasion (≥1 focus) was found to be significantly correlated with metastases and death ($P = .0071$). ([Fig. 4A-G](#)).

Applying the SEER-based risk table, we classified our cases as follows: 39 low-risk MTCs (59.1%), 16 intermediate-risk MTCs (24.2%), and 11 high-risk MTCs (16.7%). Patients classified either as intermediate- or high-risk were significantly correlated with a lower survival rate than low-risk patients ($P = .00022$). ([Fig. 5A](#)). The correlation between the SEER-based risk table and MTC patients classified according to IMTCGS showed that high-grade cases received a greater average SEER-based score than low-grade cases. Although not significant, we observed an association between the 2 scores ($P = .071$) ([Fig. 5B](#)). Finally, when we explored angioinvasion in correlation with the SEER-based risk table, patients with angioinvasion had a higher average SEER-based score than patients without angioinvasion, with a strong significant association ($P = .0002$) ([Fig. 5C](#)).

Mutational Profiling

Mutational profiling was performed by targeted sequencing of a panel of 523 genes of interest on 66 MTC samples.

Copy Number Variants

Setting a copy ratio threshold of 1.4, we identified 24 amplifications. Sixteen cases (24.2%) displayed at least 1 copy number variant (CNV), and no significant alterations were found in the remaining samples ([Supplementary Fig. S2A](#)). The *CCND1* locus was the most frequently affected, amplified in 8 (50%) CNV-altered samples (12.1% of the total cohort). CNV alterations in *FGF1*, *MYC*, and *RET* were detected in 3 samples each, corresponding to 18.8% of all CNV-altered samples and 4.5% of the entire cohort. Sporadic CNVs were also observed within the loci of *RPS6KB1*, *ERCC1*, *MYCN*, *PDGFRA*, *FGF23*, and *CHEK2*. One patient showed CNVs in 4 loci, whereas 3 samples showed co-occurrences of 2 CNVs simultaneously ([Supplementary Fig. S2B](#)). Of note, we did not analyze deletions because the approach used is not suitable for this purpose.

Microsatellite Instability and Tumor Mutation Burden

Analysis of microsatellite regions revealed very low instability, with a median microsatellite instability (MSI) percentage across the entire cohort of 1.82. Five samples (7.6%) showed MSI > 5%, and 10 samples (15.1) showed no sign of MSI ([Supplementary Fig. S2C](#)).

Tumor mutation burden (TMB) (calculated on an overall 1.13–1.28 Mb) ranged from 0 to 19.6 within the cohort, with a median of 2.35. Nine samples (13.6%) showed TMB > 5, and only 2 samples (3%) had a TMB > 10 ([Supplementary Fig. S2D](#)), reflecting an overall low genetic instability.

Small Variant Calling

After germline and low-coverage variant exclusion, 1170 coding variants were identified, including missense, frameshift, stop,

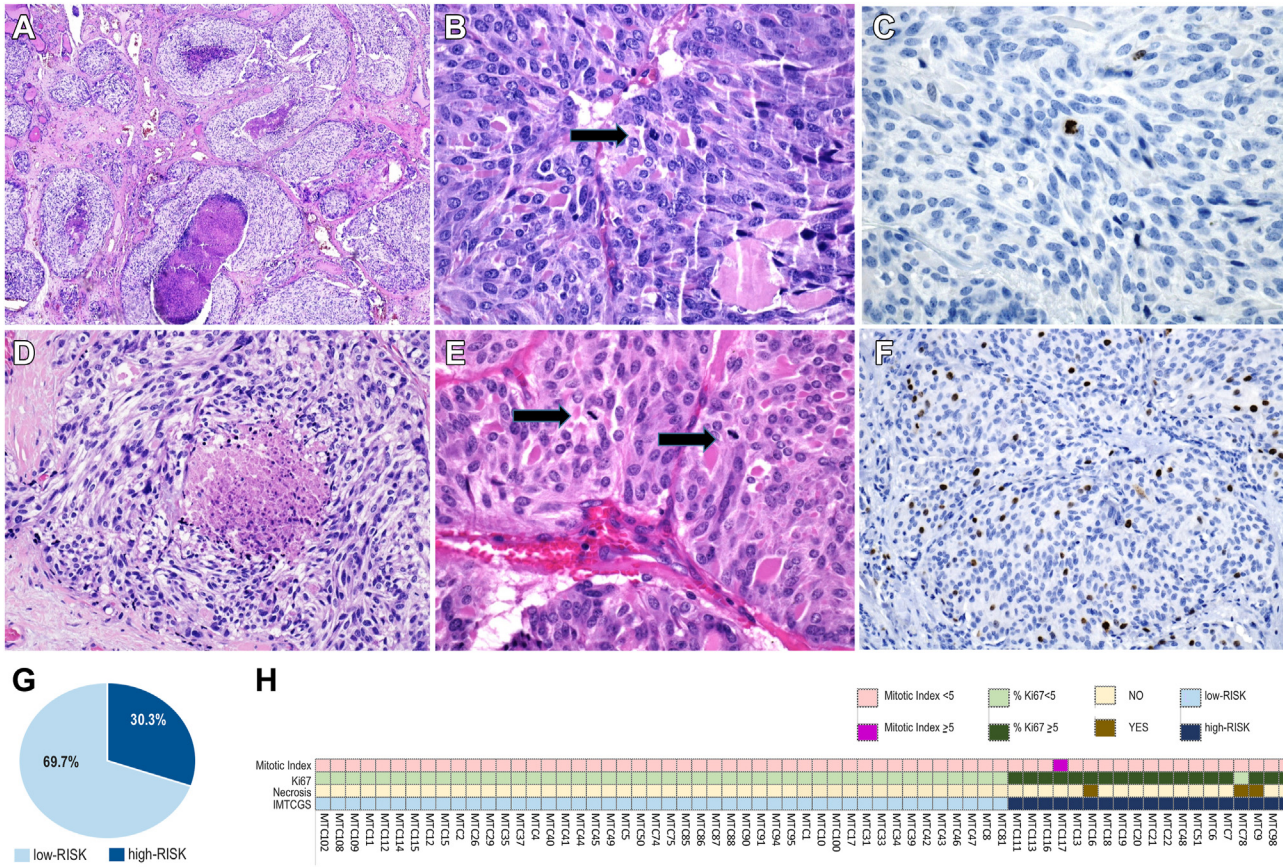


Figure 2. (A-F) Histologic criteria in the International Medullary Carcinoma Grading System (IMTCGS). Necrotic areas are often comedonic and present as aggregates of degenerated material surrounded by neoplastic cells (A, D, hematoxylin and eosin). Mitotic figures are mostly difficult to detect (B, arrow) but rarely can appear in clusters (E, arrows). The proliferative index with Ki67 is usually very low (C), but in one case, we found a Ki67 value >5% (F). (G) Pie chart of the distribution of low- and high-grade cases according to the IMTCGS in the analyzed population (66 patients). (H) Summary plot of the IMTCGS components identified in each sample.

and splicing alterations. Three hundred eighty coding variants with variant allele frequency > 3% were identified (Fig. 6A).

Most variants detected were missense mutations (65%), followed by frameshift deletions (16.1%), frameshift insertions (11.6%), in-frame deletions (5.5%), and splice site alterations (1.8%) (Fig. 6B and Supplementary Fig. S3A, B).

Focusing on the type of events, bidirectional transitions T > C and C > T were the most represented, even though the overall occurrence of transversions and transitions did not show a significant difference (Supplementary Fig. S3C).

The number of events per sample ranged from 0 to 72, with a median of 4 (Supplementary Fig. S3D). Most samples (61%) showed mutations in 1 to 5 of the analyzed genes, whereas 28% showed alterations in 6 to 20 genes (Fig. 6C). One sample (2%) showed an exceptional number of genetic alterations, with over 40 genes affected. Six (9%) of the analyzed samples did not display mutations in our analysis.

Ranking the genes according to the occurring events and setting a threshold of >5% frequency within the cohort, 20 genes were identified (Fig. 6D). As expected, *RET* was the most frequently mutated, with 37.9% (n = 25) of the samples carrying somatic alterations. *MSH3* and *CUL3* were also frequently mutated in our cohort, affecting 25.8% (n = 17) and 24.9% (n = 16) of the patients, respectively. *HRAS* mutations were detected in 12.1% (n = 8) of the samples, whereas *BRAF* mutations were found in 6.1%

(n = 4). Based on their representativeness in the overall cohort, we can assume that these 20 genes represent the MTC genetic signature.

MTC Genetic Signature Clustered Samples Into 3 Distinct Genetic Subtypes

We noted that 10 genes (50%) of the genetic signature were functionally involved in chromatin organization and function, including crucial chromatin modifiers like the polycomb group proteins *EZH2* and *ASXL1*, the lysine-specific demethylases *KDM5A* and *KDM6A*, the histone-lysine N-methyltransferase *KMT2A*, and the histone acetyltransferase *KAT6A* (Fig. 7A). Correlation analysis showed that mutations within the chromatin organizer genes showed a significant co-occurrence, but no such relationship was observed with either *HRAS* or *RET* mutations (Fig. 7B).

The genetic signature identified 3 main clusters. Cluster I comprised cases displaying mutation in *RET* or *HRAS*. Cluster II comprised cases enriched in mutation for the chromatin organizer core, and cluster III comprised samples with other sporadic variants (Fig. 7C). Noticeably, cluster II displayed a significantly higher number of mutations and higher TMB compared with the other 2 clusters, suggesting an increased genetic instability of the lesions belonging to this subset, and no significant difference in the MSI percentage was observed (Supplementary Fig. S4A, B, C).

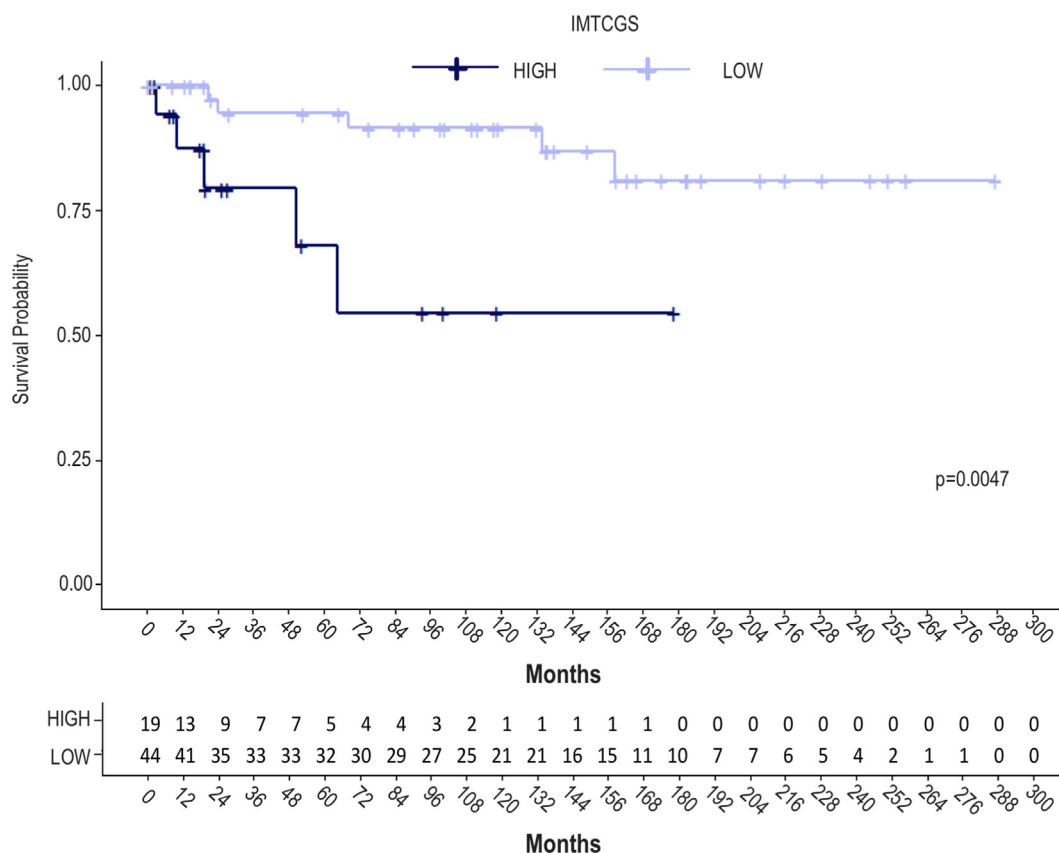


Figure 3. Kaplan-Meier curves representing event-free survival in high- and low-grade patients according to the International Medullary Carcinoma Grading System (IMTCGS). Patients classified as high-grade had a lower event-free survival probability than low-grade MTCs. The lower table reports the number of patients at risk at each time point. The P value was calculated using the log-rank test.

Correlation Analysis Between Genetic Profiling, International Medullary Carcinoma Grading System, and Surveillance, Epidemiology, and End Results-Based Risk Group

Investigating the correlation between the genetic background of MTCs and the IMTCGS, no significant association was found between TMB, CNV, MSI, the overall number of small variants, and the grading system (Supplementary Table S2). In addition, the correlation between the IMTCGS and single gene mutations did not result in any significant associations. However, considering the relationship between the genetic clusters and pathological score, cluster I contained the highest percentage of high-grade MTCs (Fig. 8A and Supplementary Fig. S4D), although this association was not statistically significant.

When we explored the impact of genetic clustering on patient outcomes, we observed that patients belonging to cluster I had a lower EFS than the others ($P = .067$) (Fig. 8B). However, in multivariate analysis considering IMTCGS and genetic clusters, only IMTCGS remained significantly associated with aggressive disease (Supplementary Fig. S5A). The greater impact of the IMTCGS on EFS was also evidenced by the Kaplan-Meier curve analysis (Fig. 8C), showing that the presence of high-grade IMTCGS defined the subclasses with the worst prognosis, regardless of genetic clusters.

No significant association was observed between genetic cluster and SEER-based risk groups (Fig. 9A). Interestingly, the combination of cluster I and high SEER-based risk characterized the group of patients with the worst prognosis, whereas no events were registered in patients in genetic clusters II-III classified at low

and intermediate SEER-based risk (Fig. 9B and Supplementary Fig. S5B).

Finally, the number of negative events was significantly associated with both genetic clustering ($P = .044$) (Fig. 10A) and SEER-based risk ($P = .004$) (Fig. 10C), with cluster I and the SEER-based high-risk group having a higher incidence of negative events. Conversely, IMTCGS classification (Fig. 10B) showed no significant correlation with negative events ($P = .262$).

Discussion

One of the main challenges in oncology is to determine accurate risk stratification of patients to enable personalized surveillance and treatment. This process mainly involves a correct histopathological diagnosis, followed by appropriate morphologic grading; however, in many oncological settings, it already needs robust molecular characterization. In MTC, the first aim has been accomplished using ancillary tools such as immunohistochemistry, and prognostic grading is likely to earn global consensus if the IMTCGS is validated by independent studies. The immediate advantage is predicting the biological risk on morphologic grounds, as already occurring for other neuroendocrine tumors, with affordable costs and good reproducibility. Genetic profiling of MTC, possibly together with morphologic grading, would benefit the grading system itself. With that in mind, we analyzed our archive selection of MTCs both morphologically and genetically.

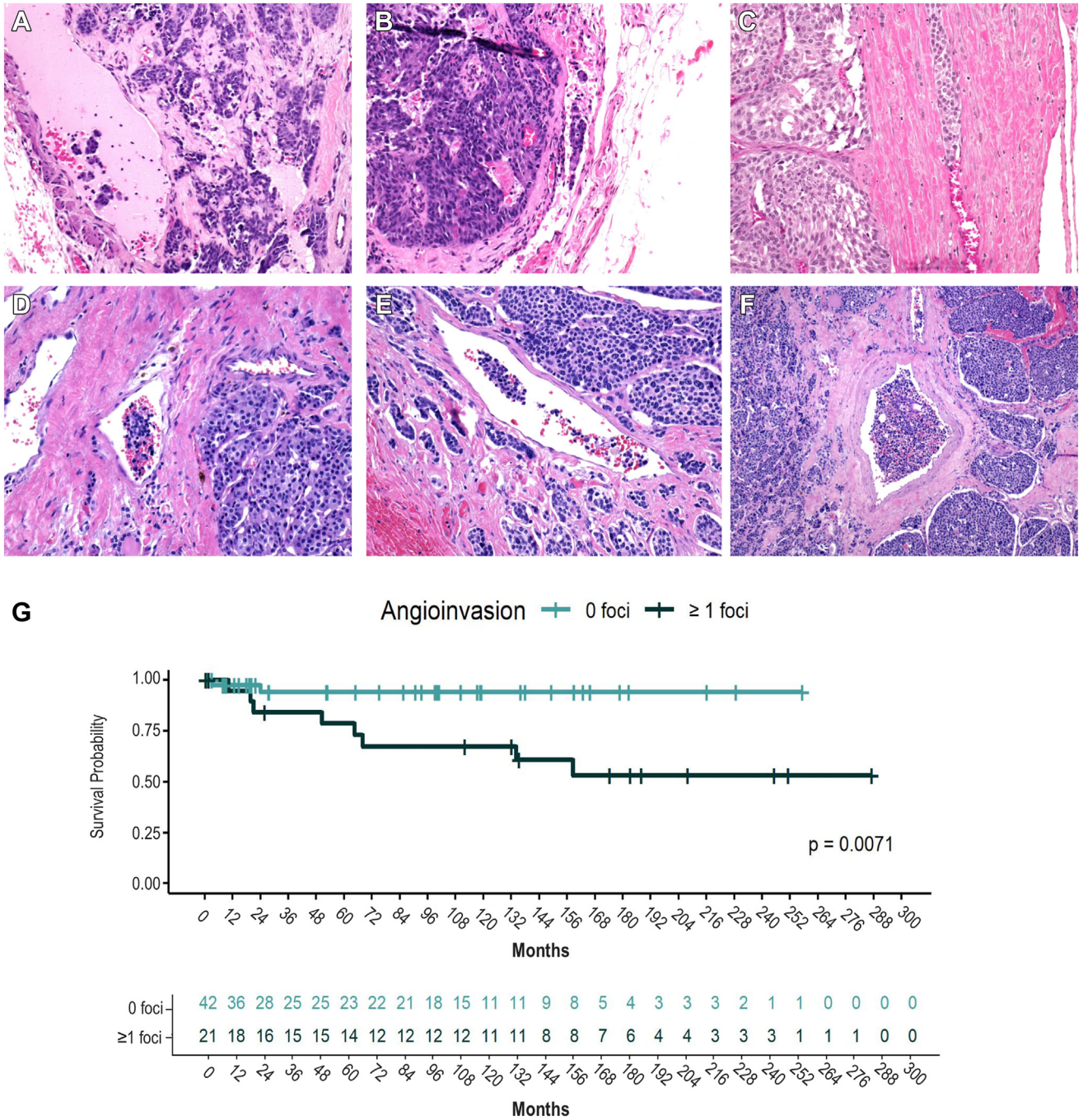


Figure 4. (A-F) Representative images of angioinvasion as neoplastic clusters intermingled with blood cells and fibrin, mainly placed in a subcapsular location (hematoxylin and eosin). (G) Kaplan-Meier curves showing that angioinvasion (≥ 1 focus) significantly correlates with metastases and death.

Histologic analysis showed that high-grade MTCs were about one-third of the cohort, confirming the results of the original paper on the IMTCGS.⁵ Although the search for necrotic areas, even inconspicuous ones, was effortless, the search for mitotic figures was often time-consuming and susceptible to interpretation bias, as is often seen in endocrine/neuroendocrine tumors.²⁸

Moreover, by selecting the hotspots, the minimum threshold for the mitotic count and different methods of scoring Ki67 values may lead to low interobserver reproducibility or differences

between small biopsies and resection specimens.^{29,30} Although recent work by Williams et al³¹ found a strong level of agreement in the assessment of grading criteria according to the IMTCGS, it is our opinion that in MTCs, where both mitotic index and Ki67 are mostly low, overestimation is an actual risk. In our series, the mitotic index was >5 in only one case (1.5%), and Ki67 was $>5\%$ in 19 cases (28.8%); necrotic areas were found only in 3 cases (4.5%). Therefore, in our series, Ki67 was numerically the main “game-decider” for assigning a tumor to either a low- or high-grade category.

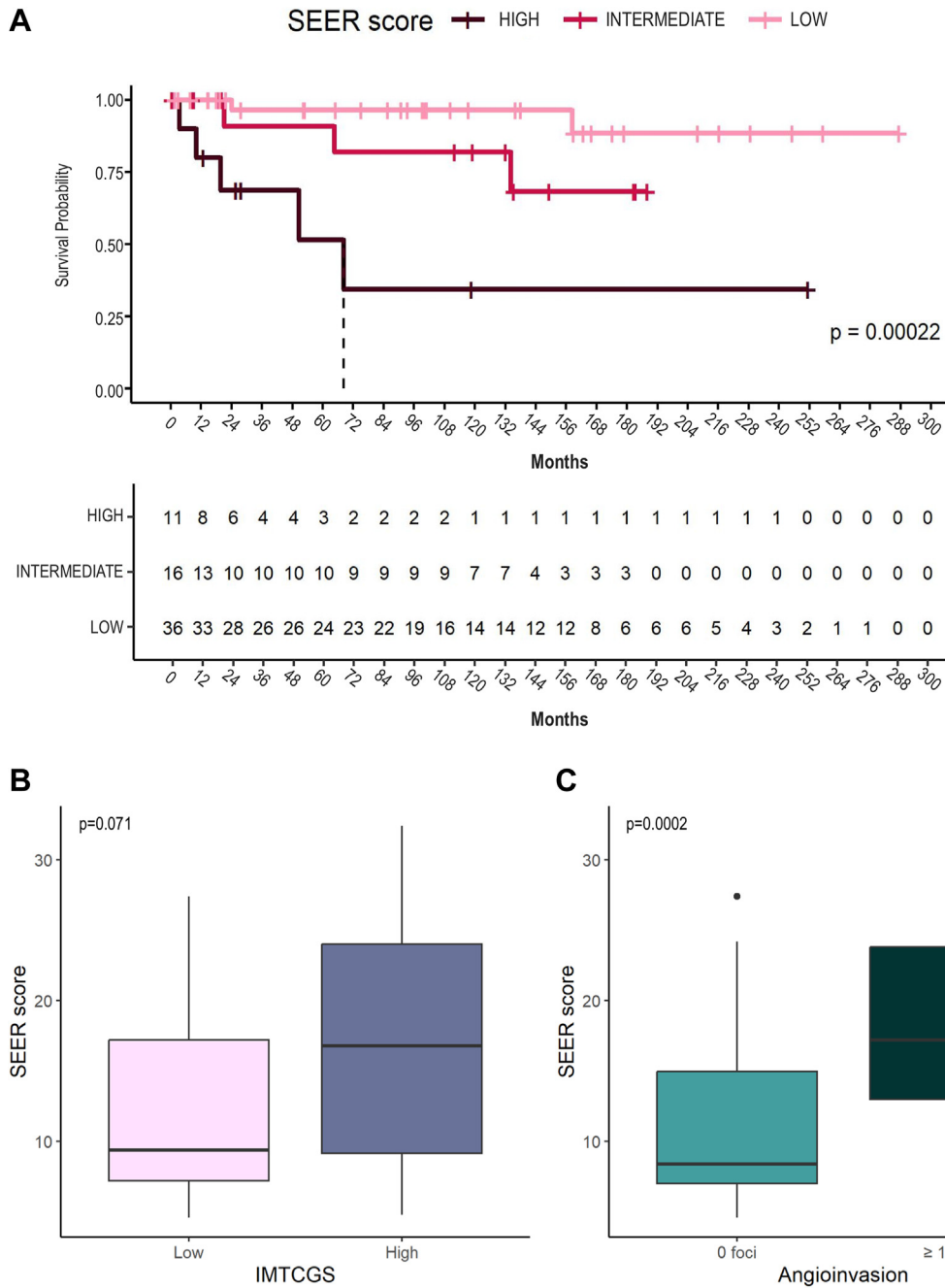


Figure 5. (A) Kaplan-Meier curves showing patients classified either as intermediate- or high-risk according to the SEER-based risk table significantly correlated with a lower survival rate than low-risk patients. The lower table reports the number of patients at risk at each time point. The *P* value was calculated using the log-rank test. (B) Box plots representing the distribution of SEER-based scores in low- and high-grade cases according to the International Medullary Carcinoma Grading System (IMTCGS). (C) Box plots correlating the distribution of SEER-based scores according to the presence of angioinvasion. SEER, Surveillance, Epidemiology, and End Results.

Grading rates among MTCs are similar in our series and in the IMTCGS (30.3% and 69.7% vs 24.8% and 75.2% for low- and high-grade cases, respectively), yet our experience is somewhat different for other variables. In particular, thyroid capsule infiltration and angioinvasion were significantly associated with metastasis or patient death. Angioinvasion is a good predictor of metastatic disease in thyroid neoplasms and it is a widely reproducible characteristic if we apply clearly accepted criteria to identify it.²⁶ However, this issue has recently been reassessed. Rios

et al¹² found that, among histologic parameters, only vascular invasion was related to relapse in 55 MTC cases. Erovic et al¹³ reported that angioinvasion was the most reliable predictor of MTC recurrence and death in 23 cases. In addition, if we stratify our cases according to SEER-based risk tables¹¹, the presence of at least one angioinvasion focus correlates with a worse prognosis (Fig. 5C). This would suggest that only cell-related variables and other well-established pathological features, especially if easily detectable like angioinvasion, might be related to the prognosis.

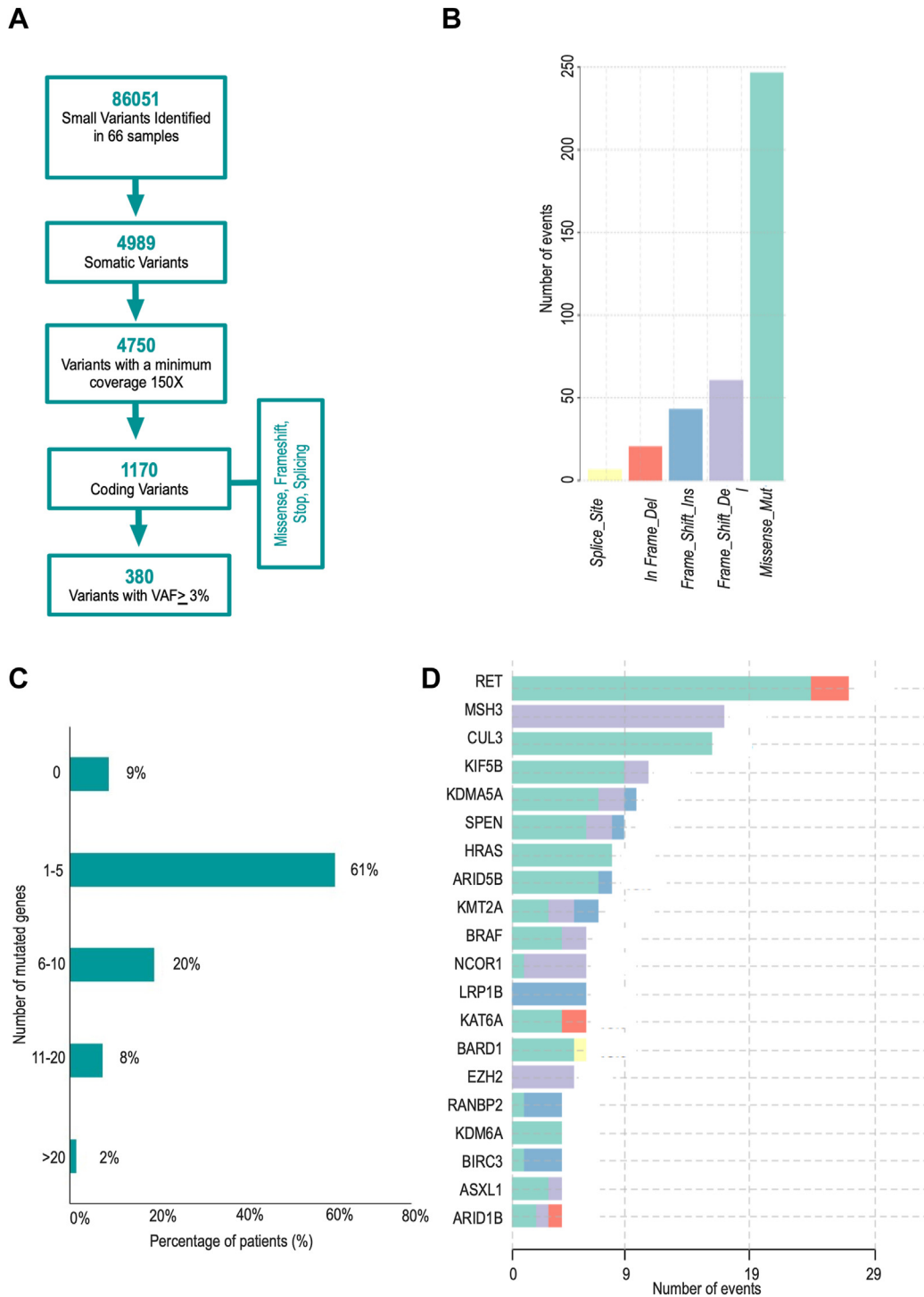


Figure 6.

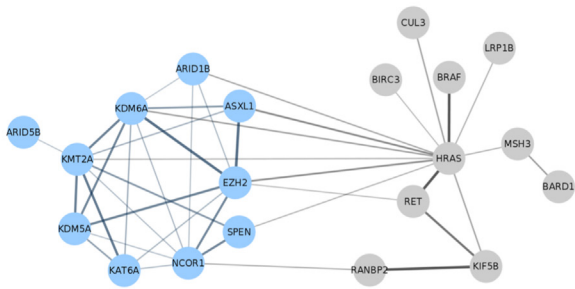
(A) Sequential criteria for the final selection of coding somatic variants based on the TruSight Oncology 500 analysis pipeline. (B) Distribution of somatic mutations identified in medullary thyroid carcinomas according to predicted functional effects. (C) Distribution of the number of mutated genes per patient. (D) Bar graph representing the total number of mutational events per gene. Colors refer to the predicted functional effect of mutations, as indicated in (B). VAF, variant allele frequency.

With the adoption of other clinical variables, such as age and sex, and more reproducible clinicopathological features, including tumor size, lymph node metastasis, and extrathyroid extension, the SEER-based metastatic risk score aims to overcome this hurdle. Thus, in our study, the SEER-based score seems a better predictor of negative events than the IMTCGS score. Therefore,

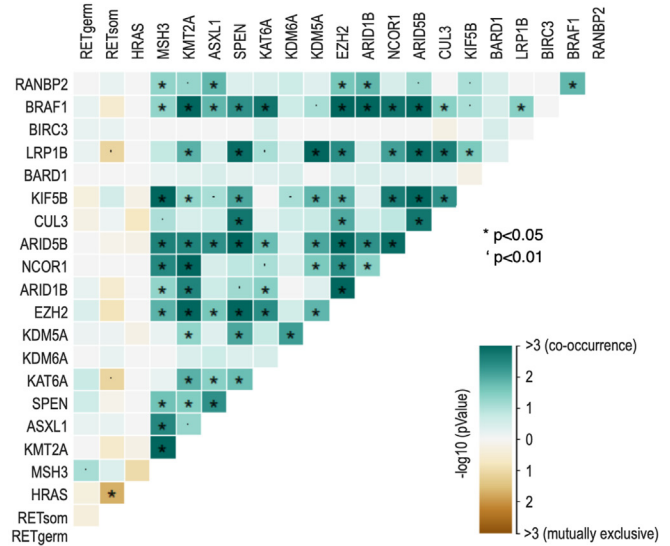
further studies on larger cohorts are needed to investigate whether all these variables could play a role in tumor evolution and patient outcome.

One of the aims of our study was to validate whether the IMTCGS represents the goal for MTC classification or just another step forward to stratify patients in a more effective and reproducible way;

A



B



C

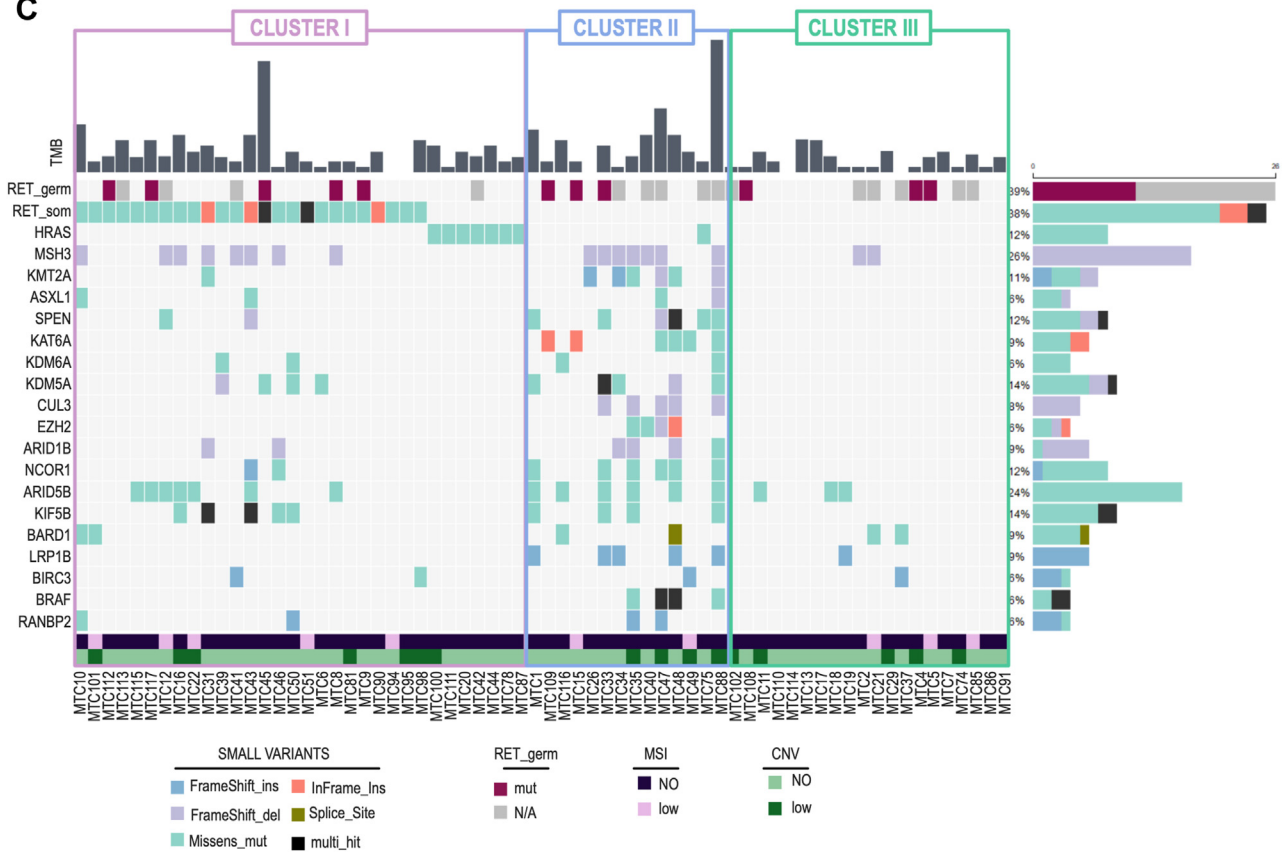


Figure 7.

(A) Cytoscape plot, including the 20 genes mutated in at least 5% of medullary thyroid carcinoma patients. Blue circles highlight the 10 interconnected genes involved in chromatin organization and function. (B) Plot representing the probability of mutually exclusive or co-occurring mutated genes. Asterisks on the plot indicate significant probability. (C) An oncoPrint representing the mutational events that occurred in each patient. Colored squares indicate different mutation types. Upper histograms represent the tumor mutational burden of each patient. The histogram on the right represents the percentage of mutated patients per gene. Lower colored bars indicate the presence of microsatellite instability and copy number variation in each patient. Boxes highlight patients classified in the same genetic cluster. Low microsatellite instability indicates a value between 1% and 10%. Low copy number variation indicates the presence of 1–4 genes.

therefore, we implemented high throughput molecular profiling and correlated the results with the IMTCGS. Combining the grading system with somatic tumor profiling could improve IMTCGS prognostication, as demonstrated in other settings.³²

We found no correlation between the IMTCGS with either genomic instability (ie, TMB, the number of small variants, MSI, or CNV) or with specific mutations. Moreover, no correlation between clustering and grading was detected, even if we indicated

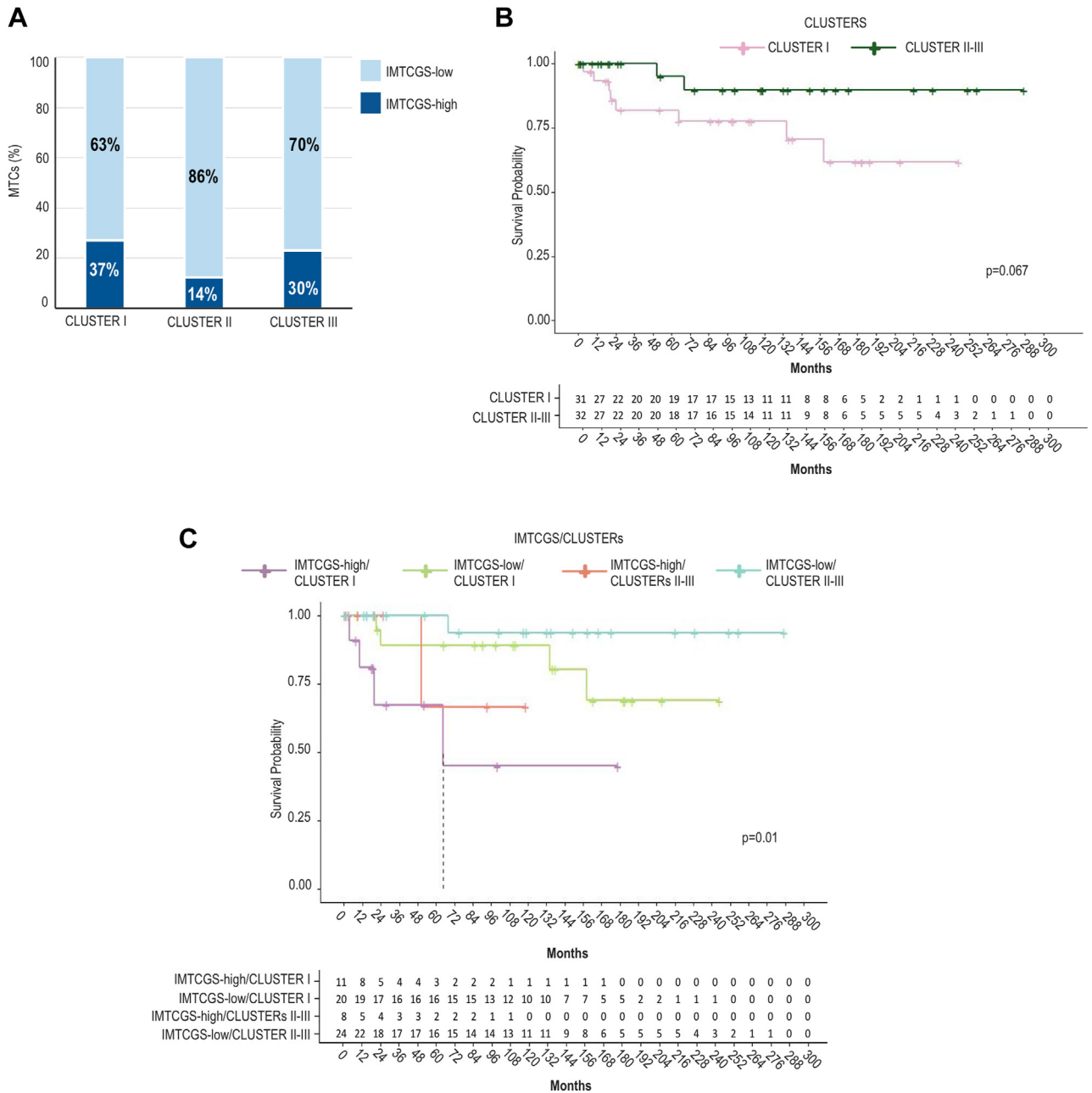


Figure 8. (A) Distribution of patients classified according to the International Medullary Carcinoma Grading System (IMTCGS) in different genetic clusters. (B) Kaplan-Meier curves representing event-free survival in cluster I vs cluster II-III patients. The lower table reports the number of patients at risk at each time point. The P value was calculated using the log-rank test. (C) Kaplan-Meier curves representing event-free survival in patients grouped by genetic cluster and IMTCGS combination. The lower table reports the number of patients at risk at each time point. The P value was calculated using the log-rank test. MTCs, medullary thyroid carcinomas.

that the presence of a specific mutational landscape characterized by alterations in either *RET* or *HRAS* concurred with grading in defining aggressiveness, probably providing additional advantages to neoplastic cells. This evidence is in line with prior reports. Indeed, previous grading schemes based on the mitotic index, Ki67, and necrosis reported no correlation with *RET* somatic mutations or *RAS* alterations in a series of 44 sporadic MTCs, even though *RET* somatic mutations are widely recognized as relevant negative prognostic factors in these lesions.³³

Several works showed that MTCs are characterized by a high incidence of private mutations besides those in *RET* and *RAS*.^{21,22,34}

Our data are in line with these observations; however, we identified a signature of 20 genes significantly altered, including *RET* and *RAS*. Ten of the 20 genes belong to a specific functional class, namely chromatin organization and function. We showed that mutations in these genes tend to co-occur and are mostly mutually exclusive with *RET* and *RAS* alterations. Alterations of key chromatin keepers, leading to profound reprogramming of the chromatin organization, may provide a possible explanation for the genetic heterogeneity of MTCs.

In addition, we report for the first time that 3 main genetic clusters can be identified according to mutation distribution.

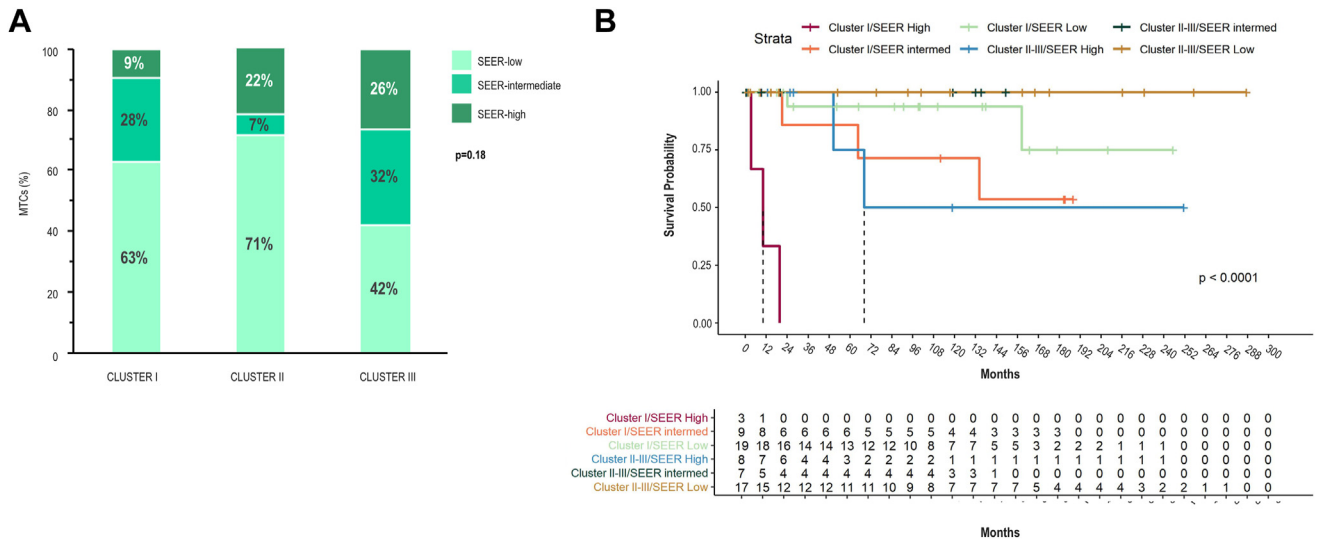


Figure 9. (A) Distribution of patients classified according to SEER-based risk table in different genetic clusters. (B) Kaplan-Meier curves representing event-free survival in patients grouped by genetic cluster and SEER-based risk groups. The lower table reports the number of patients at risk at each time point. The P value was calculated using the log-rank test. MTCs, medullary thyroid carcinomas; SEER, Surveillance, Epidemiology, and End Results.

Lesions belonging to cluster I, harboring either *RET* or *RAS* alterations, displayed reduced EFS and worse prognosis, in line with previous data. Lesions belonging to cluster II showed significantly higher TMB and overall single variant incidence, indicating a certain predisposition to increased genetic instability. However, contrary to expectations, these tumors presented quite indolent clinical behavior. The main chromatin regulators, such as the polycomb protein *EZH2*, the trithorax-group member *ASH1L*, and the histone modifiers *KDM5A*, *KDM6A*, *KMT2A*, and *KAT6A*, are known to contribute to cancer by controlling a complex gene expression program. Therefore, it would be interesting to define how mutations in these genes affect the overall transcriptional landscape of MTCs and whether such transcriptional changes may explain why lesions belonging to cluster II show apparently more indolent behavior than those of cluster I. Noticeably, Sponziello et al³⁵ investigated the expression of a panel of epigenetic regulators and the outcome and patient mutational status. They observed that the expression of *EZH2* and *SMYD3* correlated with increased aggressiveness, but it was not

influenced by mutations in either *RET* or *RAS*, supporting the hypothesis that regulators of chromatin functions may play a role in MTC biology.

In conclusion, both the IMTCGS and the SEER-based risk score showed a good prognostic performance and confirmed that most MTCs are low-grade tumors that must be kept separate from high-grade cases. Accordingly, a dichotomic distinction could be suggested, and in the near future, the classification of neuroendocrine tumors could be applied to MTCs as high-grade and low-grade C-cell neuroendocrine neoplasms of the thyroid, as already recently proposed.³⁶

Secondly, the presence of at least one angioinvasion focus was significantly correlated with metastases and death, and it should be considered in diagnosing. Finally, we provided a genetic signature of MTCs, including 3 clusters, with cluster I characterized by alterations in either *RET* or *HRAS* and concurring in defining aggressiveness. Further studies should be performed to integrate this new taxonomic approach with the molecular characterization.

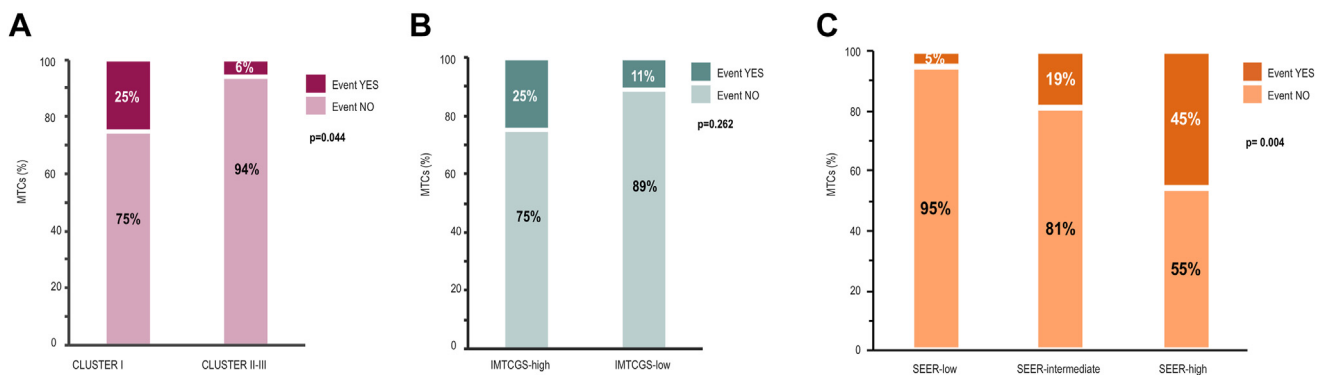


Figure 10. (A) Distribution of the number of events registered in cluster I vs cluster II-III patients. (B) The number of events in high-grade International Medullary Carcinoma Grading System (IMTCGS) vs low-grade IMTCGS patients. (C) The number of events in SEER-based risk groups. MTCs, medullary thyroid carcinomas; SEER, Surveillance, Epidemiology, and End Results.

Author Contributions

F.T., G.S., and S.P. conceived and designed the study. C.B., S.V., A.F., A.G., D.G., and D.N. provided data acquisition and analyzed and interpreted the data. F.T. provided statistical analysis. E.Z. and T.R. provided technical and material support. M.R., S.P., and A.C. wrote and revised the paper. All authors read and approved the final version of the paper.

Data Availability

All data generated or analyzed during this study are included in this published article and its supplementary information files.

Funding

This work was supported by the "Bando per la valorizzazione della Ricerca Istituzionale in ambito oncologico 2020 dell'AUSL-IRCCS di Reggio Emilia (Fondi 5 per Mille 2018)" (project code: 5M-2018-23680240) and partially supported by the Italian Ministry of Health—Ricerca Corrente Annual Program 2024.

Declaration of Competing Interest

The authors have no conflict of interest to declare.

Ethics Approval and Consent to Participate

The study was approved by the Institutional Review Board of the Azienda USL-IRCCS Reggio Emilia (protocol no.122048-2020). The study was performed in accordance with the Declaration of Helsinki.

Supplementary Material

The online version contains supplementary material available at <https://doi.org/10.1016/j.modpat.2023.100244>

References

1. Kebebew E, Ituarte PH, Siperstein AE, Duh QY, Clark OH. Medullary thyroid carcinoma: clinical characteristics, treatment, prognostic factors, and a comparison of staging systems. *Cancer*. 2000;88(5):1139–1148.
2. Roman S, Lin R, Sosa JA. Prognosis of medullary thyroid carcinoma: demographic, clinical, and pathologic predictors of survival in 1252 cases. *Cancer*. 2006;107(9):2134–2142.
3. WHO Classification of Tumours: Endocrine Tumours (ed 5), Lyon, France, International Agency for Research on Cancer; 2022.
4. Matias-Guiu X, De Lellis R. Medullary thyroid carcinoma: a 25-year perspective. *Endocr Pathol*. 2014;25(1):21–29.
5. Xu B, Fuchs TL, Ahmadi S, et al. International medullary thyroid carcinoma grading system: a validated grading system for medullary thyroid carcinoma. *J Clin Oncol*. 2022;40(1):96–104.
6. Alzumaili B, Xu B, Spanheimer PM, et al. Grading of medullary carcinoma on the basis of tumor necrosis and high mitotic rate is an independent predictor of poor outcome. *Mod Pathol*. 2020;33(9):1690–1701.
7. Fuchs TL, Nassour AJ, Glover A, et al. A proposed grading scheme for medullary thyroid carcinoma based on proliferative activity (ki67 and mitotic count) and coagulative necrosis. *Am J Surg Pathol*. 2020;44(10):1419–1428.
8. Rindi G, Klimstra DS, Abedi-Ardekani B, et al. A common classification framework for neuroendocrine neoplasms: an International Agency for Research on Cancer (IARC) and World Health Organization (WHO) expert consensus proposal. *Mod Pathol*. 2018;31(12):1770–1786.

9. Vissio E, Maletta F, Fissore J, et al. External validation of three available grading systems for medullary thyroid carcinoma in a single institution cohort. *Endocr Pathol*. 2022;33(3):359–370.
10. Podany P, Meiklejohn K, Garritano J, et al. Grading system for medullary thyroid carcinoma: an institutional experience. *Ann Diagn Pathol*. 2023;64, 152112. <https://doi.org/10.1016/j.anndiagpath.2023.152112>
11. Le M, Kawai M, Odate T, Vuong HG, Oishi N, Kondo T. Metastatic risk stratification of 2526 medullary thyroid carcinoma patients: a study based on surveillance, epidemiology, and end results database. *Endocr Pathol*. 2022;33(3):348–358.
12. Ríos A, Rodríguez JM, Acosta JM, et al. Prognostic value of histological and immunohistochemical characteristic for predicting the recurrence of medullary thyroid carcinoma. *Ann Surg Oncol*. 2010;17(9):2444–2451.
13. Erovic BM, Kim D, Cassol C, et al. Prognostic and predictive markers in medullary thyroid carcinoma. *Endocr Pathol*. 2012;23(4):232–242.
14. Elisei R, Cosci B, Romei C, et al. Prognostic significance of somatic RET oncogene mutations in sporadic medullary thyroid cancer: a 10-year follow-up study. *J Clin Endocrinol Metab*. 2008;93(3):682–687.
15. Romei C, Ugolini C, Cosci B, et al. Low prevalence of the somatic M918T RET mutation in micro-medullary thyroid cancer. *Thyroid*. 2012;22(5):476–481.
16. Romei C, Casella F, Tacito A, et al. New insights in the molecular signature of advanced medullary thyroid cancer: evidence of a bad outcome of cases with double RET mutations. *J Med Genet*. 2016;53(11):729–734.
17. Wirth LJ, Sherman E, Robinson B, et al. Efficacy of selpercatinib in RET-altered thyroid cancers. *N Engl J Med*. 2020;383(9):825–835.
18. Boichard A, Croux L, Al Ghuzlan A, et al. Somatic RAS mutations occur in a large proportion of sporadic RET-negative medullary thyroid carcinomas and extend to a previously unidentified exon. *J Clin Endocrinol Metab*. 2012;97(10):E2031–E2035.
19. Ciampi R, Romei C, Ramone T, et al. Genetic landscape of somatic mutations in a large cohort of sporadic medullary thyroid carcinomas studied by next-generation targeted sequencing. *iScience*. 2019;20:324–336.
20. Moura MM, Cavaco BM, Pinto AE, Leite V. High prevalence of RAS mutations in RET-negative sporadic medullary thyroid carcinomas. *J Clin Endocrinol Metab*. 2011;96(5):E863–E868.
21. Agrawal N, Jiao Y, Sausen M, et al. Exomic sequencing of medullary thyroid cancer reveals dominant and mutually exclusive oncogenic mutations in RET and RAS. *J Clin Endocrinol Metab*. 2013;98(2):E364–E369.
22. Simbolo M, Mian C, Barollo S, et al. High-throughput mutation profiling improves diagnostic stratification of sporadic medullary thyroid carcinomas. *Virchows Arch*. 2014;465(1):73–78.
23. Reagh J, Bullock M, Andrici J, et al. NRASQ61R mutation-specific immunohistochemistry also identifies the HRASQ61R mutation in medullary thyroid cancer and may have a role in triaging genetic testing for MEN2. *Am J Surg Pathol*. 2017;41(1):75–81.
24. Ji JH, Oh YL, Hong M, et al. Identification of driving ALK fusion genes and genomic landscape of medullary thyroid cancer. *PLoS Genet*. 2015;11(8):e1005467.
25. Cree IA, Tan PH, Travis WD, et al. Counting mitoses: Sl(ze) matters. *Mod Pathol*. 2021;34(9):1651–1657.
26. Mete O, Asa SL. Pathological definition and clinical significance of vascular invasion in thyroid carcinomas of follicular epithelial derivation. *Mod Pathol*. 2011;24(12):1545–1552.
27. Mayakonda A, Lin DC, Assenov Y, Plass C, Koeffler HP. Maftools: efficient and comprehensive analysis of somatic variants in cancer. *Genome Res*. 2018;28(11):1747–1756.
28. Huang W, Nebiolo C, Esbona K, Hu R, Lloyd R. Ki67 index and mitotic count: correlation and variables affecting the accuracy of the quantification in endocrine/neuroendocrine tumors. *Ann Diagn Pathol*. 2020;48, 151586.
29. Walts AE, Ines D, Marchevsky AM. Limited role of Ki-67 proliferative index in predicting overall short-term survival in patients with typical and atypical pulmonary carcinoid tumors. *Mod Pathol*. 2012;25(9):1258–1264.
30. Boland JM, Kroneman TN, Jenkins SM, et al. Ki-67 labeling index in pulmonary carcinoid tumors: comparison between small biopsy and resection using tumor tracing and hot spot methods. *Arch Pathol Lab Med*. 2020;144:982–990.
31. Williams JF, Zhao M, Najdawi F, et al. Grading of medullary thyroid carcinoma: an interobserver reproducibility study. *Endocr Pathol*. 2022;33(3):371–377.
32. Wachtel H, Hutchens T, Baraban E, et al. Predicting metastatic potential in pheochromocytoma and paraganglioma: a comparison of PASS and GAPP scoring systems. *J Clin Endocrinol Metab*. 2020;105(12):e4661–e4670.
33. Najdawi F, Ahmadi S, Capelletti M, Dong F, Chau NG, Barletta JA. Evaluation of grade in a genotyped cohort of sporadic medullary thyroid carcinomas. *Histopathology*. 2021;79(3):427–436.
34. Heilmann AM, Subbiah V, Wang K, et al. Comprehensive genomic profiling of clinically advanced medullary thyroid carcinoma. *Oncology*. 2016;90(6):339–346.
35. Sponziello M, Durante C, Boichard A, et al. Epigenetic-related gene expression profile in medullary thyroid cancer revealed the overexpression of the histone methyltransferases EZH2 and SMYD3 in aggressive tumours. *Mol Cell Endocrinol*. 2014;392(1-2):8–13.
36. Jung CK, Agarwal S, Hang J, Lim D, Bychkov A, Mete O. Update on C-cell neuroendocrine neoplasm: prognostic and predictive histopathologic and molecular features of medullary thyroid carcinoma. *Endocr Pathol*. 2023;34(1):1–22.